Slotted Patch Antenna with Wide Bandwidth for In-body Biotelemetry Applications

Piyush Kumar Mishra, Keshav Mathur, and Vijay Shanker Tripathi

Motilal Nehru National Institute of Technology Allahabad, Prayagraj, India

https://doi.org/10.26636/jtit.2024.2.1412

Abstract — This paper proposes a slotted patch antenna with wide bandwidth covering ISM frequency band (2.40–2.48 GHz) for implantable biotelemetry applications. A homogeneous skin phantom (HSP) model proves the usability of the proposed antenna in in-body environments. At a resonance frequency of 2.42 GHz, the design shows an S_{11} parameter of –35.56 dB, a percentage impedance bandwidth of 66.6% (2–4 GHz), and the maximum peak gain of –24.80 dBi. To validate the simulated results, the designed antenna was fabricated and measured, showing good compliance with the expected results. To ensure tissue safety, a specific absorption rate (SAR) is simulated for the proposed antenna which satisfies the requirements of IEEE standards, with a value of 87.75 W/kg for 10 g of tissue. The proposed antenna shows a telemetry range of 11 and 6.3 m at 7 kbps and 100 kbps data rates, respectively. The key features of the proposed antenna include the following: miniaturization, good S parameters, wide bandwidth, low SAR, good telemetry range, and high gain.

Keywords — biotelemetry, implantable antenna, ISM band, specific absorption rate (SAR)

1. Introduction

Implantable medical devices (IMD) are receiving more attention from researchers and are used for monitoring human health. IMDs sense real-time data and interact with an external device wirelessly. Hence, implanted antennas need to be used in IMDs to transmit data to the receiver [1], [2]. A wideband antenna offering features that allowing it to be implanted is a key element for a such communication system [3]. Designs of implantable antennas differ from those of free space antennas, since they are surrounded by lossy human tissue, influencing the antenna's characteristics. When designing an implantable antenna, a few key points need to be considered, such as compactness, wide bandwidth, biocompatibility, patient safety, etc.

Several frequency bands are allowed in implantable applications, such as ISM, MICS or WMTS. The MICS band is mainly allocated and preferred for implantable applications, but it has some limitations, for instance narrow bandwidth and low data transmission rate. The ISM band has become increasingly attractive for implantable applications, as it offers a number of advantages, including wide frequency bandwidth, fast data transmission, circuit simplicity, ability to incorporate small antenna architectures, and good tissue penetration by radio waves. The 2.4–2.48 GHz ISM band is the most popular selection for wireless in-body biomedical devices due to good availability of commercial off-the-shelf (COTS) components.

Antennas proposed for such wireless biomedical devices are usually dipole, microstrip, spiral, meandered or dielectric resonator antennas to ensure sufficient miniaturization. Researchers have designed a number of different types of implantable antennas for biotelemetry applications, as presented in papers [4]–[6], [9]–[20]. In [4], a meander-shaped patch aerial was proposed for IMDs. The designed antenna covers 7.3% of the 2.4 GHz ISM bandwidth. In [5], a serpentine-shaped patch and an open-ended ground plane-based antenna were designed for the 2.40 GHz ISM bandwidth, covering 8.6% thereof. A slot antenna was also designed for biotelemetry applications, covering 23.9% of the MICS band, as described in paper [6].

One of the essential requirements of implanted antennas is their stability of performance inside the human body. Surrounding human tissues affect the resonance frequency of the antenna and cause an uncontrolled shift, known as the detuning effect. Therefore, antennas offering as great a bandwidth as possible are needed to mitigate this effect. For bandwidth enhancement, an aperture-coupled dielectric-loaded implantable antenna was proposed in [12] for the 2.4 GHz ISM band, offering good bandwidth coverage (22%) and a low SAR value. In [14], a stacked parasitic structure was used for increasing the bandwidth. The achieved impedance bandwidth was 30%.

A wideband compact implantable antenna for the 2.4 GHz ISM band was presented in [16], with its bandwidth coverage equaling 29%, i.e. approximately 670 MHz. In [20], a miniature implantable antenna was shown, relying on low permittivity substrate (RT Duroid 5880, $\varepsilon_r = 2.2$). This design offered a 64.9% wide impedance bandwidth.

Due to designed ground structure of the antennas mentioned above, undesired backward radiation causes a reduction in their performance, manifesting itself in energy efficiency and gain losses. The bandwidth of the reported antennas needs to be improved as well. Therefore, in this work, a center rectangular slotted patch antenna with a full ground plane, offering high impedance bandwidth is proposed. To achieve

Tab. 1. Optimized antenna parameter values.

Parameter	Value [mm]	Parameter	Value [mm]
l_p	10	l_3	1
w_p	10	r_o	1.20
w_1	0.25	r_i	0.50
s_1	1.25	g_w	4.40
s_2	1.50	g_l	7.90
s_3	5	r_s	1
s_w	5	l_b	35
r_1	0.50	w_b	70
l_2	1.25	d	6

the highest possible degree of miniaturization, the shorting pins technique is used.

2. Design Methodology

For the purpose of implanting the antenna, a design with a resonating frequency of ISM 2.42 GHz is considered.

2.1. Antenna Design

Figure 1 shows the dimensions and shape of the antenna. The Rogers 6010 ($\varepsilon_r = 10.2$, $\mathrm{tg}\,\delta = 0.0023$) PCB laminate with a thickness of $h = 0.25$ mm is chosen for the substrate and the superstrate layer, as the antenna is expected to operate while being surrounded by human tissue. A full ground plane is used to reduce backward radiation, which leads to efficiency and gain improvements. The center slot of 5 × 5 mm helps fix the operating frequency within the ISM band, resulting in resonance at 3.9 GHz. By inserting such a square center slot, the effective size of the patch is reduced and the surface current path becomes longer than with a regular shape patch.

Next, more slots are introduced to enhance the surface current route and to get closer to resonance in the ISM band. By introducing circular slots at the corners of the square center slot, the resonance frequency is lowered to 3.0 GHz, while 2 shorting pins, each with a radius of 0.5 mm, shorting the patch to the ground provide a satisfactory value of resonant frequency equaling 2.42 GHz and an acceptable gain value.

The final design of antenna this work is concerned with has a volume of 50 mm^3 and measures 10 × 10 × 0.50 mm. Table 1 summarizes all the dimensions of the patch, ground, and other aerial structures.

2.2. Simulation Setup

The designed antenna was simulated using the Ansoft HFSS software, with the finite element approach adopted and a homogeneous human skin tissue box model, with its dimensions equaling 70 × 70 × 35 mm^3. The frequency-dependent electrical parameters of skin in the 2.4 GHz ISM band ($\varepsilon_r = 38$, $\sigma = 1.44$ S/m) were taken from [7], and the design is simulated at various skin depths, as shown in Fig. 3b.

3. Results and Discussion

In the next step, the designed antenna was fabricated and then its parameters were measured to validate the simulated results. The prototype of the antenna and the measurement setup are presented in Fig. 4. To ensure that the measurements are taken under conditions similar to those under human skin, the antenna was placed between two layers of pork [11]. The S parameter is measured by using a vector network analyzer (VNA) and an anechoic chamber was used for far-field measurements.

Figure 5a shows the simulated and measured values of the S parameter vs. frequency, where $|S_{11}|$ value equals –35.55 dB at 2.42 GHz. The measured bandwidth of the designed antenna, covered by a pork tissue sample, is 1.31 GHz (2.06–3.37 GHz). One may notice that the measured results fail to perfectly match the simulated parameters. This is caused by many factors impacting the simulation and measurement environments, such as accuracy of simulation and measurement tools, complexity of biological tissues, tissue properties (as these may not accurately represent the specific conditions which were used for simulation), physical fabrication and placement of the antenna in the pork tissue during measurements, frequency ranges, and the power levels used during simulation and measurement phases. From Fig. 5a, it can also be observed that the measured parameters of the designed antenna nearly match the simulated values and also holds the 2.40 GHz ISM band.

The far-field gain plot of the designed antenna is shown in Fig. 5b. The design shows a simulated peak gain of –24.80 dBi and a measured peak gain of –25.07 dBi, respectively, at the working frequency of 2.42 GHz. Negative gain is observed because the designed antenna is electrically tiny and is surrounded by lossy skin tissue. It is observed that all implanted patch antennas offer low gain values. Compared to other reference antennas, the designed aerial shows a good gain value due to the full ground feature, which results in low backward radiation.

Figure 5c shows the simulated and measured radiation patterns at the working frequency of 2.42 GHz. One may notice that the E and H plane graphs are almost omnidirectional. The maximum simulated and measured radiation values amount to –7.04 dB and –9.79 dB, respectively, corresponding to bore side direction, i.e. $\theta = 0°$.

The surface current density and SAR are also simulated to examine the impact of the designed antenna on human tissue. Figure 6a shows the surface current density on the patch with a maximum value of 173.75 A/m, while Fig. 6b illustrates the average SAR distribution for 10-grams of tissue at 2.41 GHz resonance frequency. SAR analysis is conducted by calculating the amount of heat the radiation generates in the human tissue. The IEEE C95.1-2019 standard specifies the allowed SAR value of 2 W/kg per 10 g of tissue in the frequency range of 100 kHz to 6 GHz for implantable patch antennas [8].

To validate this, the proposed antenna was inserted into a homogeneous skin box structure, at a depth of 6 mm. At

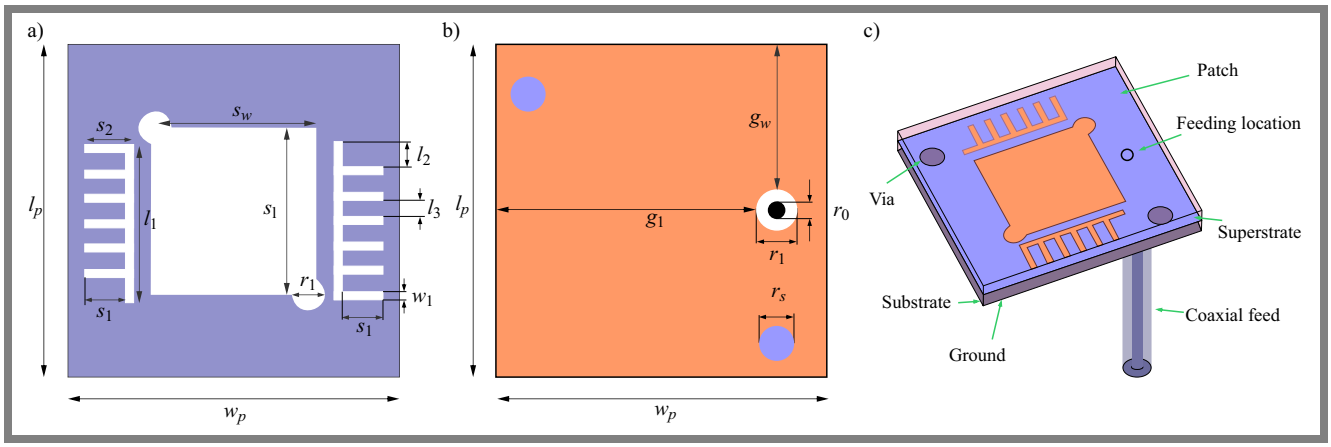

Fig. 1. Details of the designed IMD antenna: a) top, b) bottom, and c) isometric view.

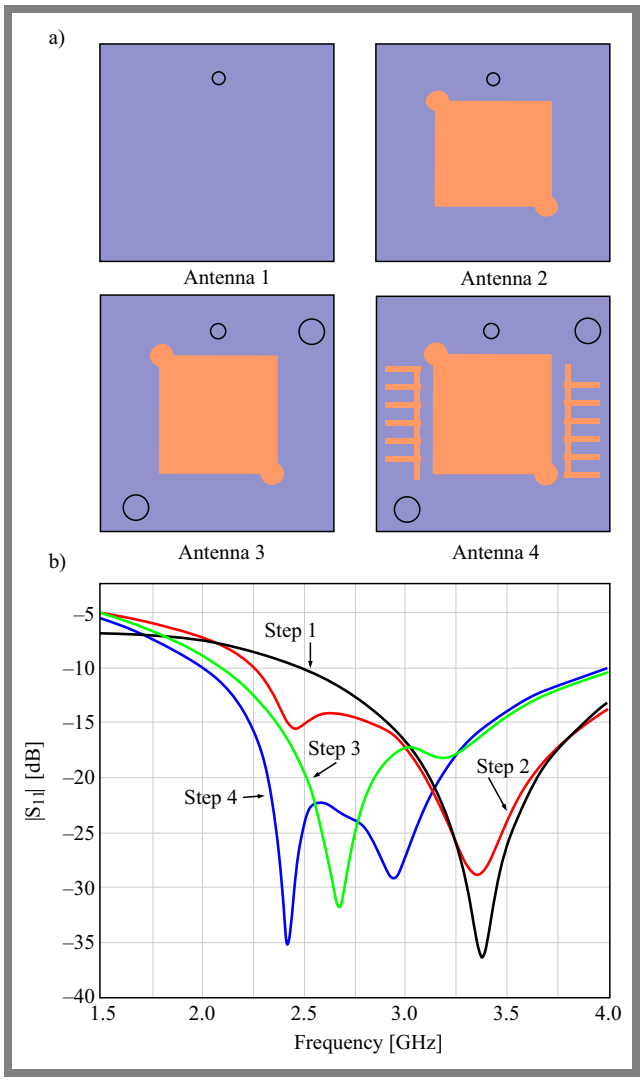

Fig. 2. Four design steps and plot showing the corresponding S parameters of the designed antenna.

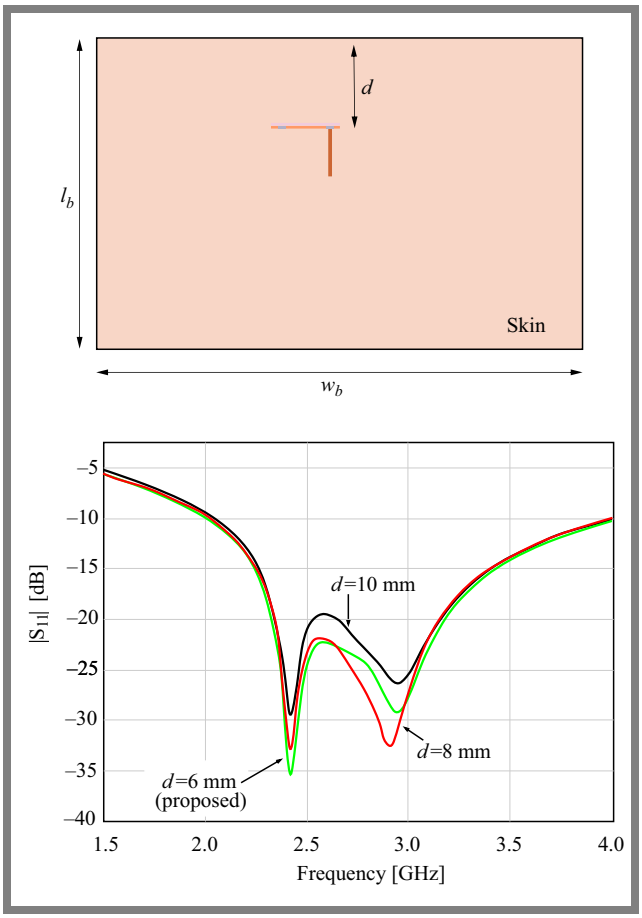

Fig. 3. Homogeneous skin box model – a) and S parameters at different skin box depths – b).

input power of 1 W, the SAR value, as shown in Fig. 6b, reached 87.75 W/kg for 10 g of tissue. Therefore the input power limit equals 22.79 mW. It is much higher than the minimum required input power of 25 μW, showing that the calculated SAR value is not an issue for this design.

4. Link Budget Calculation

In the next step, link budget calculations are performed to obtain the telemetry range of the proposed antenna at different data rates. The link margin for far-field communication should be typically over 0 dB, which basically balances all

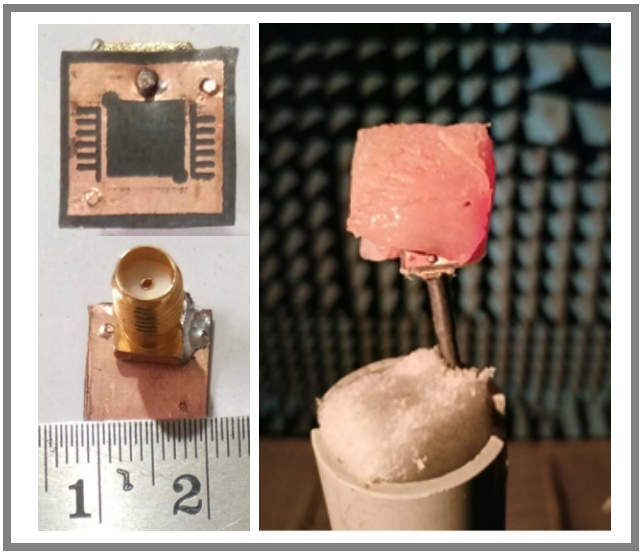

Fig. 4. Prototype of the designed antenna and the measurement setup.

the losses and the gain of the communication link. The link margin equation and parameters are taken from [2] and are summarized in Tab. 2:

$$Link\ margin\ \ [\mathrm{dB}] = Link\frac{C}{N_0} - Required\frac{C}{N_0}$$

$$LM\ [\mathrm{dB}] = P_t + G_t - L_f + G_r - N_0 - \frac{E_b}{N_0} - 10\log B_r + G_c - G_d,$$

where P_t is transmitted power, G_t is transmitted gain, L_f is free space path loss, G_r is receiver gain, B_r is data rate, and N_0 is noise power density. The free space path loss L_f can be calculated as:

$$L_f[\mathrm{dB}] = 20\log\frac{4\pi d}{\lambda}.$$

Link margin is calculated for two data rates of 7 kbps and 100 kbps, and the corresponding link margin vs. distance plot is obtained (Fig. 7).

From Fig. 7, one may observe that the proposed antenna supports communication up to a distance of 11 m and 6.2 m, for 7 kbps and 100 kbps data rates, respectively.

A comparison of the proposed antenna and other designs described in recent papers is provided in Tab. 3. One may notice that the obtained bandwidth of the designed antenna is better than the values obtained while using other referenced antennas. From the table, one may also see that other parameters of the proposed antenna are satisfactory as well and that it may be useful in implant applications.

5. Conclusion

A skin-implanted antenna operating within the 2.4 GHz ISM band has been presented in this paper. The design has an excellent bandwidth of 2 GHz and a reflection coefficient $|S_{11}|$ of –35.55 dB at resonance frequency of 2.42 GHz. To confirm the simulated results, the antenna's parameters were measured

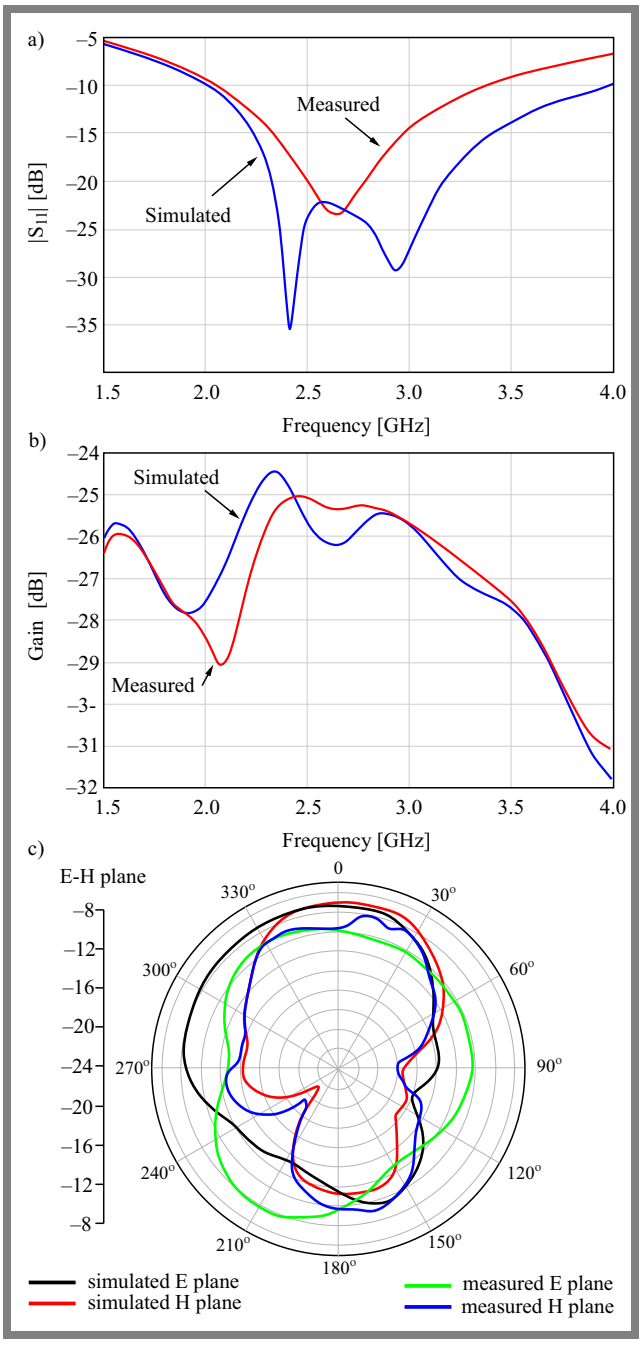

Fig. 5. Summary of simulated and measured parameters: a) S parameter, b) far field gain, and c) radiation pattern of the designed antenna on an E–H plane.

under conditions similar to a real implant, and the results have been found to be satisfactory. SAR values are determined according to several IEEE standards for safety purposes, with the results being well under the permissible values. It should be highlighted that the proposed antenna has a wide impedance bandwidth, low SAR, good gain, and a frequency spectrum that is suitable for biomedical applications.

Finally, the maximum allowed input power was calculated, and it was observed that the full permissible input power was much higher than the value of 25 µW required for the transmitter. The link budget analysis proved that a telemetry range of up to 11 m and 6.2 m could be achieved for the

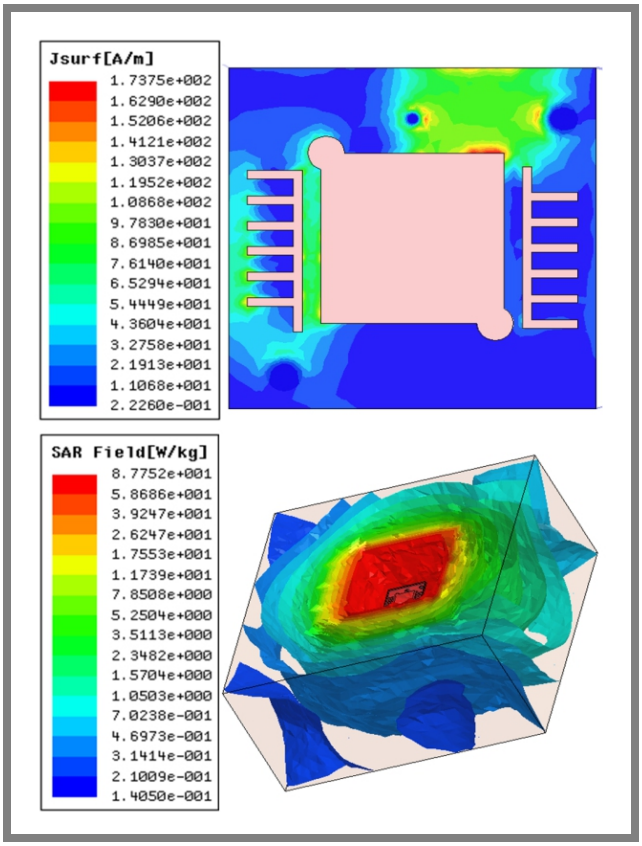

Fig. 6. Surface current on patch a) and average SAR for 10 g tissue at 2.41 GHz b).

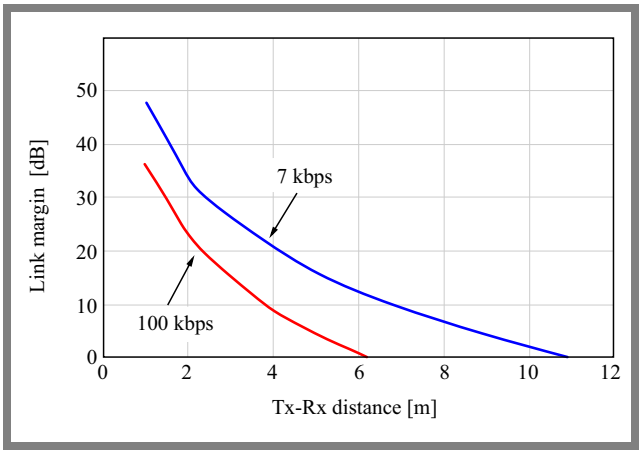

Fig. 7. Link margin plot for 7 kbps and 100 kbps.

data rates of 7 kbps and 100 kbps, respectively. The obtained results of the antenna that has been designed and fabricated for the purposes of this paper suggest that it may be successfully used in biotelemetry applications.

Tab. 2. Parameters used for the link budget analysis.

Parameter	Value
Frequency	2.42 GHz
T_x power	–40 dBm
T_x gain (G_t)	–24.80 dBi
G_r	2.15
N_0	–199.95
$\frac{E_b}{N_0}$	9.6
B_r	7 and 100 kbps
G_c	0
G_d	2.5

References

[1] S.A.A. Shah and H. Yoo, "Scalp-Implantable Antenna Systems for Intracranial Pressure Monitoring", *IEEE Transactions on Antennas and Propagation*, vol. 66, no. 4, pp. 2170–2173, 2018 (https://doi.org/10.1109/TAP.2018.2801346).

[2] C. Liu, Y. Guo, and S. Xiao, "Capacitively Loaded Circularly Polarized Implantable Patch Antenna for ISM Band Biomedical Applications", *IEEE Transactions on Antennas and Propagation*, vol. 62, no. 5, pp. 2407–2417, 2014 (https://doi.org/10.1109/TAP.2014.2307341).

[3] M. Samsuzzaman, M.T. Islam, and M.R.I. Faruque, "Dual-band Multi Slot Patch Antenna for Wireless Applications", *Journal of Telecommunications and Information Technology*, no. 2, pp. 19–23, 2013 (https://jtit.pl/jtit/article/view/1211).

[4] M. Zada and H. Yoo, "A Miniaturized Triple-band Implantable Antenna System for Bio-telemetry Applications", *IEEE Transactions on Antennas and Propagation*, vol. 66, no. 12, pp. 7378–7382, 2018 (https://doi.org/10.1109/TAP.2018.2874681).

[5] Y. Cho and H. Yoo, "Miniaturized Dual-band Implantable Antenna for Wireless Biotelemetry", *IEEE Electronics Letters*, vol. 52, no. 12, pp. 1005–1007, 2016 (https://doi.org/10.1049/el.2016.10510).

[6] C. Liu, Y.-X. Guo, and S. Xiao, "A Hybrid Patch/Slot Implantable Antenna for Biotelemetry Devices", *IEEE Antennas and Wireless Propagation Letters*, vol. 11, pp. 1646–1649, 2012 (https://doi.org/10.1109/LAWP.2013.2237879).

[7] S. Gabriel, E. Corthoutand, and C. Gabriel, "Dielectric Properties of Biological Tissues" *Physics in Medicine and Biology*, vol. 41, no. 11, pp. 2231–2293, 1996 (https://doi.org/10.1088/0031-9155/41/11/001).

[8] IEEE Std C95.1-2019, "IEEE Standard for Safety Levels with Respect to Human Exposure to Electric, Magnetic, and Electromagnetic Fields, 0 Hz to 300 GHz", 2019 (https://doi.org/10.1109/IEEESTD.2019.8859679).

[9] Y. Liu, Y. Chen, H. Lin, and F.H. Juwono, "A Novel Differentially Fed Compact Dual-band Implantable Antenna for Biotelemetry Applications", *IEEE Antennas and Wireless Propagation Letters*, vol. 15, pp. 1791–1794, 2016 (https://doi.org/10.1109/LAWP.2016.2536735).

[10] P.K. Mishra, S. Raj, and V.S. Tripathi, "A Novel Skin-implantable Patch Antenna for Biomedical Applications", in: *2020 IEEE 7th Uttar Pradesh Section International Conference on Electrical, Electronics and Computer Engineering (UPCON)*, Prayagraj, India, 2020 (https://doi.org/10.1109/UPCON50219.2020.9376443).

[11] Z. Xia *et al.*, "A Wideband Circularly Polarized Implantable Patch Antenna for ISM Band Biomedical Applications", *IEEE Transactions on Antennas and Propagation*, vol. 68, no. 3, pp. 2399–2404, 2020 (https://doi.org/10.1109/TAP.2019.2944538).

[12] P.K. Mishra and V.S. Tripathi, "A Miniature Dielectric Loaded Wide Band Circularly Polarized Implantable Antenna with Low Specific Absorption Rate for Biomedical Applications", *International Journal of FR and Microwave Computer-Aided Engineering*, vol. 32, no. 8, art. no. 23227, 2022 (https://doi.org/10.1002/mmce.23227).

[13] A. Pal, P.K. Mishra, and V.S. Tripathi, "A Circularly Polarized Wideband Implantable Patch Antenna for Biomedical Applications", *International Journal of Microwave and Wireless Technologies*, vol. 15, no. 6, pp. 1075–1081, 2022 (https://doi.org/10.1017/S1759078722001052).

Tab. 3. Comparison of the proposed antenna with other designs.

Reference	Volume [mm^3]	Frequency [GHz]	Implantation environment				BW [%]	Gain [dBi]	SAR [W/kg]
			Body tissue	Shape	Phantom dimensions [mm^3]	Depth [mm]			
[1]	24	2.40	Skin	Cube	200 × 200 × 200	4	8.57	–22.80	102.04
[4]	21	2.45	Skin	Cube	200 × 200 × 200	4.5	7.30	–20.40	40.3
[5]	31.5	2.45	Skin	Cube	200 × 200 × 200	3	8.60	–21.20	59.0
[9]	642.62	2.40	Skin	Cube	100 × 100 × 100	4	6.60	–27.10	–
[10]	127	2.45	Skin	Cuboid	90 × 90 × 25	4	23.21	–16.20	63.0
[11]	121.98	2.4	Skin	Cuboid	90 × 90 × 26	3	21.50	–33.00	90.0
[12]	102	2.44	Skin	Cuboid	80 × 80 × 25	4	22.00	–28.96	2.19
[13]	50	2.45	Skin	Cuboid	90 × 90 × 25	4	49.75	–28.12	58.01
[16]	60.5	2.45	Muscle	Cuboid	60 × 60 × 40	2	29.00	–24.00	78.86
This work	50	2.42	Skin	Cuboid	70 × 70 × 35	6	66.66	–24.80	87.75

[14] D. Jing, H. Li, X. Ding, W. Shao, and S. Xiao, "Compact and Broadband Circularly Polarized Implantable Antenna for Wireless Implantable Medical Devices", *IEEE Antennas and Wireless Propagation Letters*, vol. 22, no. 6, pp. 1236–1240, 2023 (https://doi.org/10.1109/LAWP.2023.3237558).

[15] J. Zhang *et al.*, "Compact Dual-Band Implantable Antenna for Wireless Biotelemetry in Arteriovenous Grafts", *IEEE Transactions on Antennas and Propagation*, vol. 71, no. 6, pp. 4759–4771, 2023 (https://doi.org/10.1109/TAP.2023.3266786).

[16] A.Z.A. Zaki *et al.*, "Design and Modeling of Ultra-Compact Wideband Implantable Antenna for Wireless ISM Band", *Bioengineering*, vol. 10, no. 2, art. no. 216, 2023 (https://doi.org/10.3390/bioengineering10020216).

[17] S.N. Shah *et al.*, "Dual-Band Two-Port MIMO Antenna for Biomedical Deep Tissue Communication: Design, Characterization, and Performance Analysis", *IEEE Access*, vol. 11, pp. 104622–104632, 2023 (https://doi.org/10.1109/ACCESS.2023.3319216).

[18] R.-X. Ou and W.-L. Yu, "Design of Small Circular Polarized Antenna with Ring Descriptive Loading for Biomedical Applications", *IEEE Access*, vol. 11, pp. 130840–130849, 2023 (https://doi.org/10.1109/ACCESS.2023.3333362).

[19] M.S. Zulkefli *et al.*, "Experimental Wireless Link and SAR Assessments of an Implantable PIFA for Biotelemetry in the 2.45 GHz Band", *IEEE Journal of Electromagnetics, RF and Microwaves in Medicine and Biology*, vol. 7, no. 3, pp. 281–289, 2023 (https://doi.org/10.1109/JERM.2023.3294707).

[20] P. Mohanraj and P.R. Selvakumaran, "Compact Wideband Implantable Antenna for Biomedical Applications", *Current Applied Physics*, vol. 43, pp. 50–56, 2022 (https://doi.org/10.1016/j.cap.2022.08.007).

Piyush Kumar Mishra, Ph.D. Student
Electronics and Communication Engineering Department
https://orcid.org/0000-0002-6206-0450
E-mail: pmishra@mnnit.ac.in
Motilal Nehru National Institute of Technology Allahabad, Prayagraj, India
http://www.mnnit.ac.in

Keshav Mathur, M.Tech. Student
Electronics and Communication Engineering Department
https://orcid.org/0009-0007-2844-8842
E-mail: keshav.2020cm12@mnnit.ac.in
Motilal Nehru National Institute of Technology Allahabad, Prayagraj, India
http://www.mnnit.ac.in

Vijay Shanker Tripathi, Professor
Electronics and Communication Engineering Department
https://orcid.org/0000-0002-0575-8174
E-mail: vst@mnnit.ac.in
Motilal Nehru National Institute of Technology Allahabad, Prayagraj, India
http://www.mnnit.ac.in